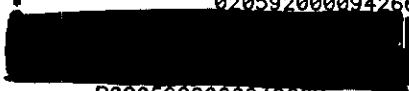


CEBAF-PR-87-006 VWC3 ✓  
V.D. Burkert  
Spin Degrees of Freedom Region  
02059200094266



02059200094266

*Master Copy*



0205 9100 002 806 8

CEBAF-PR-87-006

SPIN DEGREES OF FREEDOM IN ELECTRON NUCLEON  
SCATTERING IN THE RESONANCE REGION

*Volker D. Burkert*  
*Continuous Electron Beam Accelerator Facility*  
*12070 Jefferson Avenue*  
*Newport News, VA 23606*

SPIN DEGREES OF FREEDOM IN ELECTRON NUCLEON  
SCATTERING IN THE RESONANCE REGION

Volker D. Burkert  
CEBAF  
12070 Jefferson Avenue  
Newport News, VA 23606, USA

Abstract

Some aspects of using polarized electrons and/or polarized targets in electron-nucleon scattering experiments are discussed. Polarization measurements can be used to extend the knowledge of nucleon form-factor measurements to higher  $Q^2$  and are indispensable for a model-independent extraction of the helicity amplitudes of exclusive meson production. Measurements of polarization asymmetries may also help in revealing the excitation of weaker resonances.

I. Introduction

The study of the electromagnetic couplings of the ground state nucleon and its excited states should be an essential part of any research program to investigate electroweak interactions with nuclei. The ultimate goal in studying the 'elementary' process is to obtain information on the  $\gamma NN^*$  vertex. Detailed knowledge of this transition provides the data base which is necessary for the interpretation of electron nucleus scattering at high momentum and high energy transfer. The understanding of nucleon-nucleon correlation, e.g., will depend essentially upon our understanding of the role played by nucleon resonances in nuclei. Studying nucleon resonance transition is, on the other hand, very important in itself. The knowledge of the  $Q^2$  dependence of the  $\gamma NN^*$  transition appears crucial for the development of more realistic, QCD based, interquark potentials for light quarks, and finally for the definite implementation of QCD to hadrons at intermediate distances where non perturbative effects have to be taken into account.

II. The Electric Formfactor of the Neutron and the Proton

The hadronic current in elastic electron nucleon scattering is specified by the electric and magnetic formfactors  $G_E(Q^2)$  and  $G_M(Q^2)$ . The knowledge of these quantities up to the highest possible  $Q^2$  is not only of fundamental importance for testing microscopic models of the nucleon and its electromagnetic coupling, but has strong impact on the interpretation of electron nucleus scattering in general. Our present knowledge is practically limited to the magnetic formfactors  $|G_{Mp}|$  and  $|G_{Mn}|$  which have been measured for  $Q^2$  up to 30 and 20  $\text{GeV}^2$ , respectively.  $G_{Ep}$  has been measured up to 3  $\text{GeV}^2$  with uncertainties between 10% and 30% at  $Q^2 > 1 \text{GeV}^2$ . Little is known about the electric formfactor of the neutron. In fact, our only solid knowledge comes from scattering of thermal neutrons off electrons from atoms, showing that  $dG_{En}/dQ^2 > 0$  at  $Q^2 \rightarrow 0$ . There is some information on  $G_{En}$  at  $Q^2 < 1 \text{GeV}^2$ , extracted from elastic eD scattering<sup>1</sup>. These results, however, are necessarily model dependent in that they depend on the specific deuteron wavefunction assumed in the analysis. Attempts to measure  $|G_{En}|$  from quasielastic eD scattering have not yielded satisfactory results<sup>2</sup>. A model independent measurement of  $G_{En}$  is urgently needed. Studying quark effects in nuclei at large  $Q^2$  will bear heavily on the knowledge of the nucleon form-

factors, since new effects will reveal themselves as deviations from the "conventional" picture of the nucleus.

Several ways of measuring this fundamental quantity have been proposed. One way is to measure  $G_{En}$  in scattering of polarized electrons from unpolarized neutrons and to study the neutron recoil polarization in a second scattering experiment. An alternative method is to use quasielastic scattering of polarized electrons from vector polarized deuterium<sup>3</sup>. I will briefly discuss this latter method which may be of interest not only for use in storage rings but for external beam experiments at Bates and CEBAF as well.

For an orientation of the neutron spin in the electron scattering plane perpendicular to the direction of  $\vec{y}$ , the elastic electron neutron cross section is given by:

$$\frac{d\sigma}{d\Omega} = \left(\frac{d\sigma}{d\Omega}\right)_0 \left[1 + P_e P_n A^n(Q^2)\right]$$

( $P_e$  = electron polarization,  $P_n$  = effective neutron polarization,  $(d\sigma/d\Omega)_0$  = unpolarized<sup>n</sup> cross section). The asymmetry is given by:

$$A^n(Q^2) = \frac{2 G_{En} G_{Mn} \sqrt{\tau(1+\tau)} \text{tg} \frac{\theta_e}{2}}{G_{En}^2 + \tau G_{Mn}^2 + 2\tau^2(1+\tau) G_{Mn}^2 \text{tg}^2 \frac{\theta_e}{2}} ; \tau = \frac{Q^2}{4M_n^2}$$

The appearance of the interference term allows the measurement of  $G_{En}$  if  $G_{Mn}$  is known, without Rosenbluth separation. This is advantageous in determining the electric formfactor because  $G_{En}$  is expected to be small<sup>4</sup>, and its contribution to the elastic cross section at large  $Q^2$  is negligible. Fig. 1 shows the expected asymmetry for  $G_{En} = 0$  and  $G_{Mn} = -\tau G_{Mp}/\mu$ , both of which are consistent with present data at not too small  $Q^2$ .

1. An Experiment to Measure  $G_{En}$  in  $d(\vec{e}, e' n)p$

Using a polarized ND<sub>2</sub> solid state target with an approximately 20mW cooling power at a temperature of  $\approx 270\text{mK}$ , luminosities of  $\approx 0.6 \cdot 10^{22} \text{ cm}^{-2} \text{ sec}^{-1}$  have been obtained (only neutrons in deuterium are counted)<sup>5</sup>. A cooling power of  $\approx 500\text{mW}$  was achieved at  $\approx 270\text{mK}$  in a dilution refrigerator<sup>6</sup>. This would allow measurements to be performed with effective luminosities in excess of  $10^{22} \text{ cm}^{-2} \text{ sec}^{-1}$ . Neutron polarizations of  $\approx 45\%$  were obtained in a 3.5T magnetic field<sup>7</sup>. With a 5T field, neutron polarizations of 60% can be anticipated. Using appropriate kinematical cuts on the scattered electron and the recoil neutron angle, background contributions from neutrons in the nitrogen nucleus can largely be suppressed, and effective polarizations of  $\approx 40\%$  should be achievable<sup>8</sup>. The expected running time of a measurement of  $G_{En}$  is shown in Fig. 2 for a specific experimental setup. It is perhaps worthwhile noting that the use of polarized deuterium as target material has the advantage of allowing the same measurement to be carried out with protons (from the deuterons). A comparison of proton measurements with ND<sub>2</sub> and NH<sub>3</sub> as target materials would allow the testing of effects which may result from the binding of the proton in the deuteron. This information provides a sensitive mean in correcting the neutron data for nuclear effects.

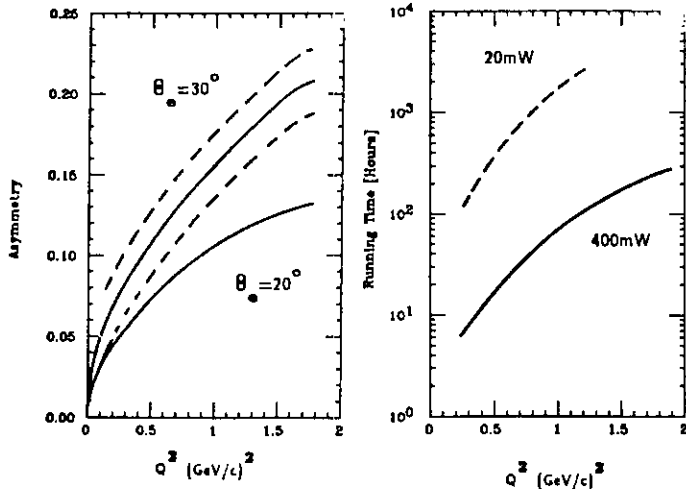


Fig. 1 Polarization asymmetry  $n(\vec{e}, en)$  for electron scattering angles.  $G_{En} = -\tau G_{Mn} / \mu_n$  has been assumed.  $A = 0$  if  $G_{En} = 0$ . The dashed lines indicate an uncertainty  $\delta A = \pm 0.02$ .

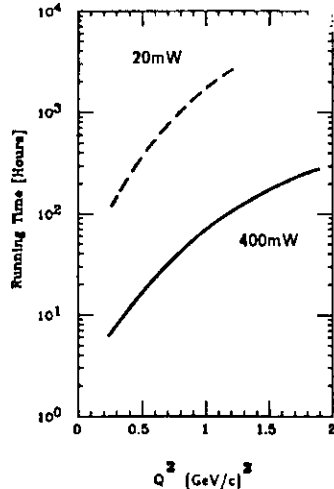


Fig. 2 Running time for an experiment to measure the neutron asymmetry with  $\delta A = \pm 0.02$ , for polarized target cryostats with different cooling power.

## 2. An Experiment to Measure $G_{Ep}$ in $\vec{p}(\vec{e}, e'p)$

The method outlined above can also be used to measure the polarized proton asymmetry using  $NH_3$  as polarized target material. Hence the electric formfactor  $G_{Ep}$  of the proton can be measured. Since protons can be polarized to a higher degree than deuterons at higher temperatures, polarized proton targets can be operated at much higher cooling powers and therefore can be used with higher electron currents. With a  ${}^4\text{He}$  cryostate of  $\approx 10$  Watts of cooling power at 1 Kelvin, luminosities of  $5 \cdot 10^{24} \text{ cm}^{-2} \text{ sec}^{-1}$  (only free protons count) can be achieved<sup>18</sup>. The polarization asymmetry as predicted by QCD sum rule calculations<sup>5</sup> is shown in Fig. 3. The expected running time of an experiment to measure  $G_{Ep}$  is displayed in Fig. 4. Measurements of  $G_{Ep}$  for  $Q^2$  up to  $6 \text{ GeV}^2$  appear feasible using existing polarized target technology.

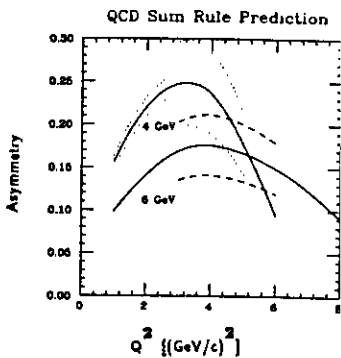


Fig. 3 QCD sum rule prediction of the polarized  $\vec{p}(\vec{e}, ep)$  asymmetry.

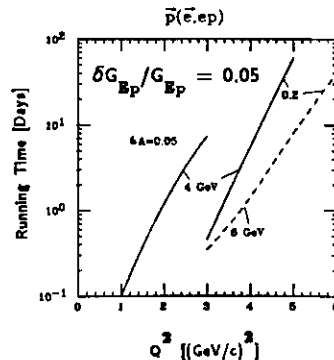


Fig. 4 Expected running time for an experiment to measure  $G_{Ep}$  with  $\pm 5\%$  and  $\pm 20\%$ , respectively.

In summary, it appears that with presently available polarized solid state target technology, considerably higher  $Q^2$  values can be reached in measuring the electric proton and neutron formfactors than has been possible with the usual Rosenbluth separation.

## III. Electroproduction of Nucleon Resonances

Studying the  $Q^2$  dependence of the  $\gamma NN^*$  transition for the nucleon resonances gives us many details of the wavefunction of the excited states. This knowledge is essential in developing more realistic interquark potentials which are based on the fundamentals of QCD<sup>11</sup>. It appears important to obtain as much information as possible to probe the full electromagnetic structure of the transition, including its spin structure. Before discussing exclusive measurements in some detail, it is perhaps instructive to recall some features of the inclusive cross section in the resonance region.

### 1. The Inclusive Cross Section $p(e, e')X$

It is widely assumed that the cross section for electroproduction of nucleon resonances would decrease faster with increasing  $Q^2$  than the nonresonant part does. This, however, turns out not to be the case, as can be inferred from Fig. 5, where the total photoabsorption cross section in the mass region up to  $W \approx 2 \text{ GeV}$  is shown for small and large values of  $Q^2$ <sup>12</sup>. I want to point out several interesting features in the  $Q^2$  dependence of the cross section:

- The strong enhancement in the region of the  $\Lambda(1232)$  disappears quickly at large  $Q^2$ .
- The enhancements near  $W \approx 1.5 \text{ GeV}$  and  $W \approx 1.7 \text{ GeV}$  remain prominent up to the highest  $Q^2$ . The signal/background ratio does not appear to decrease at all over the entire  $Q^2$  range.
- The shoulder near  $W \approx 1.45 \text{ GeV}$  in the  $Q^2 = 0$  data, which is generally attributed to the excitation of the Roper  $P_{11}(1440)$ , disappears very quickly with  $Q^2$ . Already at  $Q^2 = 0.1 \text{ GeV}^2$  there are no indications of an excitation of this resonance any more.
- At  $Q^2 > 3 \text{ GeV}^2$  a resonant structure near  $W \approx 1.4 \text{ GeV}$  seems to emerge which may even become dominant over the  $\Lambda(1232)$  at the highest  $Q^2$ .

In conclusion, the total photoabsorption cross section indicates very different  $Q^2$  dependences for the various resonant parts of the cross section. The fast decrease of the  $\Lambda(1232)$  excitation strength offers the possibility to study the lower mass region at large  $Q^2$  in detail, where the cross section is no longer dominated by the higher mass tail of the  $\Lambda(1232)$ . This may prove especially important for studying the excitation of the  $P_{11}(1440)$  and possible other  $P_{11}$  partners nearby.

It is obvious that due to the large widths and large number of resonances (approximately 20 with masses below  $2 \text{ GeV}$ ) individual resonances can in general not be isolated<sup>18</sup>. A program to separate and study details of single resonances requires studying spin and isospin structure of the intermediate state which can only be done by measuring the resonance decay products in exclusive experiments.

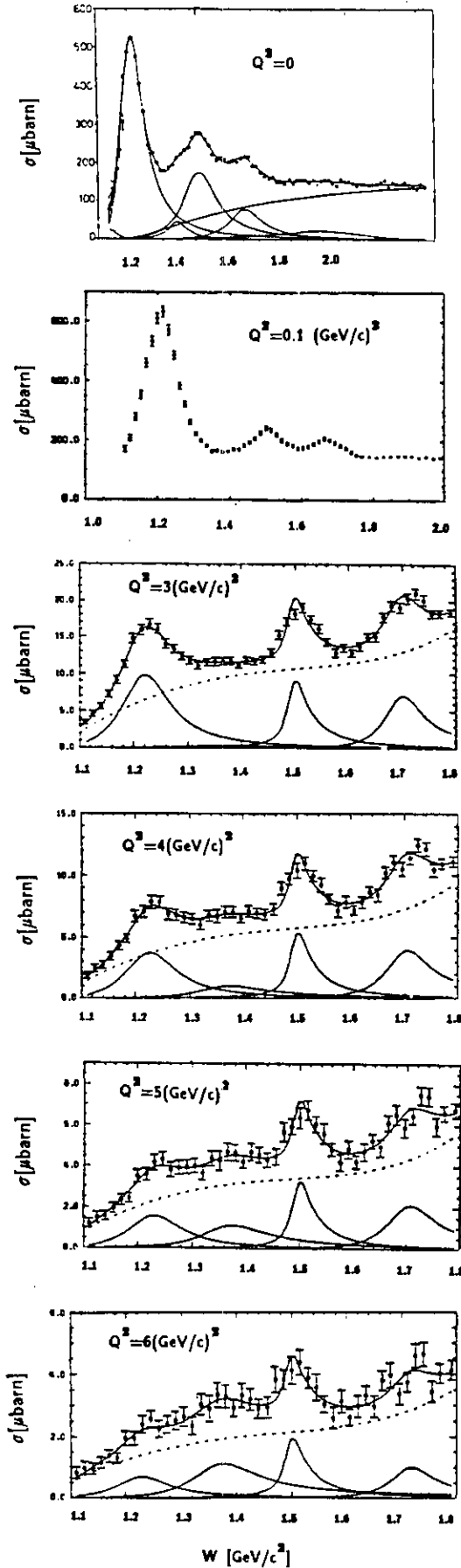


Fig. 5 Inclusive cross section for  $p(e,e')x$  at fixed  $Q^2$ .

## 2. Exclusive Reactions for Resonance Studies

Many of the lower lying resonances have a strong single  $\pi$  or  $\eta$  decay channel. The reactions  $p(e,e'p)\pi^0(\eta)$ ,  $p(e,e'\pi^+)n$  and  $n(e,e'\pi^-)p$  are therefore most suitable for studying resonance properties. The unpolarized coincidence cross section is given by

$$\frac{d\sigma}{dE_e d\Omega_e d\Omega_\pi} = \Gamma_T \left( \sigma_T + \epsilon \sigma_L + \epsilon \sigma_{TT} \cos 2\phi + \sqrt{\epsilon(1+\epsilon)/2} \sigma_{TL} \cos \phi \right)$$

The first and third term depend on the transverse unpolarized and polarized coupling of the photon, the second term depends on the the longitudinal part and the last term is a transverse/longitudinal interference term. These quantities are functions of  $Q^2$ ,  $W$ ,  $\theta^*$  and can be expressed in terms of 6 complex, parity conserving helicity amplitudes<sup>14</sup>:

$$\begin{aligned} \sigma_T &= P/2K \left[ |H_1|^2 + |H_2|^2 + |H_3|^2 + |H_4|^2 \right] \\ \sigma_L &= P/2K \left[ |H_5|^2 + |H_6|^2 \right] \\ \sigma_{TT} &= P/K \operatorname{Re} \left[ H_2 H_3^* - H_1 H_4^* \right] \\ \sigma_{TL} &= 2P/K \operatorname{Re} \left[ H_5^* (H_1 - H_4) + H_6^* (H_2 + H_3) \right] \end{aligned}$$

A complete and model independent determination of these amplitudes requires at least 11 independent measurements at each kinematical point. Unpolarized experiments allow four independent measurements only. With a polarized beam one additional combination of these amplitudes can be measured. A polarized nucleon target allows eight sensible measurements, and experiments with polarized beams and polarized target allow measurement of five more combinations of amplitudes<sup>15</sup>. If one can measure the recoil polarization, e.g., if the final state nucleon is a proton, one can obtain the same number of combinations as with a polarized target, four of which are different from the polarized target case<sup>16</sup>.

A separation of the various terms requires detailed out-of-plane measurements. In addition to the  $\cos\phi$  and  $\cos 2\phi$  terms of the unpolarized cross section  $\sin\phi$  and  $\sin 2\phi$  terms appear in the polarization dependent terms. Also, measurements with different orientations of the target spin will be necessary.

## 3. Existing Data

Although such a detailed experimental program has not been conducted so far, some information, in particular on the most prominent resonances, has been obtained from measuring the angular dependence of the unpolarized coincidence cross section. From experiments performed at the BONN, DESY, NINA synchrotrons<sup>12,9</sup> we have limited information on the transverse helicity amplitudes  $A_{1/2}$  and  $A_{3/2}$  for the  $P_{11}(1232)$ ,  $S_{11}(1535)$ ,  $D_{13}(1520)$  and the  $F_{15}(1688)$  proton resonances. It is well known that the  $\gamma p P_{11}(1232)$  transition amplitudes drop faster with  $Q^2$  than the elastic formfactor. As can be inferred from Fig. 6, the other resonances show quite a different behaviour.

The  $S_{11}(1535)$  which can only be excited by helicity 1/2 in the  $\gamma p$  initial state exhibits a strikingly weak  $Q^2$  dependence. At  $Q^2=3 \text{ GeV}^2$ , the  $A_{1/2}$  has decreased by only 50% of its value at  $Q^2=0$ . For the  $D_{13}(1520)$  and the  $F_{15}(1688)$  the helicity-3/2 dominance at  $Q^2=0$  switches to a helicity-1/2 dominance at large  $Q^2$ , a behaviour that is qualitatively in accordance with quark model predictions<sup>11</sup>, as well as with expectations

from helicity conservation in perturbative QCD<sup>17</sup>. The transition to helicity 1/2 dominance seems to be a general feature at high  $Q^2$ . It is the details, however, of how this transition occurs that would give us insight into the dynamics of the multi-quark-gluon system. Very little information is available for resonances other than the ones mentioned above, and practically no data exist for neutron resonances.

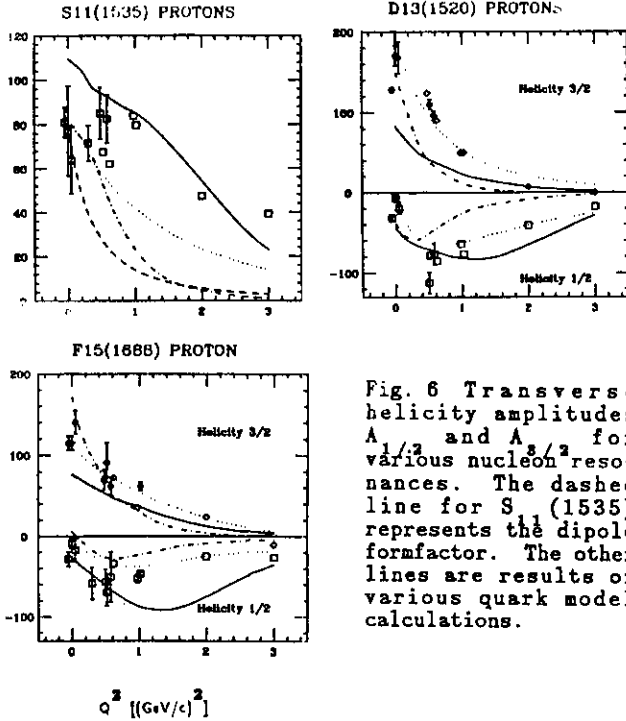


Fig. 6 Transverse helicity amplitudes  $A_{1/2}$  and  $A_{3/2}$  for various nucleon resonances. The dashed line for  $S_{11}(1535)$  represents the dipole formfactor. The other lines are results of various quark model calculations.

It should be noted that the data points in Fig. 6 are subject to systematic uncertainties, largely due to the limited experimental information that could be used in the data analysis. Also, there are uncertainties in the description of the nonresonant part of the cross section<sup>12</sup>.

An experimental program to study electroproduction of nucleon resonances should be able to combine very high statistics unpolarized cross section measurements and detailed polarization measurements of the relevant asymmetries, going up to the highest possible  $Q^2$ . Polarization asymmetries contain interference terms of amplitudes. They are therefore especially sensitive to small amplitudes and to relative phases between amplitudes. Already information of limited statistical accuracy will prove extremely sensitive in determining signs and absolute values of the less prominent amplitudes. In the following chapter we give two examples to illustrate the sensitivity of polarization asymmetries to small amplitudes.

#### 4. The Scalar Amplitude $S_{1+}$ in the $\gamma, p \Delta(1232)$ Transition

Quark models with SU(6) symmetry yield  $S_{1+} = 0$  for the scalar (longitudinal) multipole as a consequence of the assumed pure magnetic dipole transition between two states with angular momentum  $L=0$  of the 3 quark system. The inclusion of a hyperfine color magnetic interaction arising from the QCD motivated one gluon exchange between the valence quarks<sup>18</sup> leads to a finite longitudinal coupling, reflecting the (SU(6) forbidden)  $L=2$  state of the multi-quark wavefunction<sup>19</sup>. Our present knowledge on  $S_{1+}$  for the  $\Delta(1232)$  comes from studying  $p(e, e')\pi^0$ . Assuming s and p wave contributions only,

and  $M_{1+}$  dominance (only terms with  $M_{1+}$  are retained), the unpolarized cross section can be written as:

$$\begin{aligned} \frac{d\sigma}{d\Omega} \approx & \left[ \frac{5}{2} |M_{1+}|^2 - 3 \operatorname{Re}(M_{1+}E_{1+}^*) + \operatorname{Re}(M_{1+}M_{1-}^*) \right] \\ & + \cos\theta_{\pi}^* \left[ 2 \operatorname{Re}(E_{0+}M_{1+}^*) \right] \\ & + \cos^2\theta_{\pi}^* \left[ -\frac{3}{2} |M_{1+}|^2 + 9 \operatorname{Re}(M_{1+}E_{1+}^*) - 3 \operatorname{Re}(M_{1-}M_{1+}^*) \right] \\ & + \epsilon \sin^2\theta_{\pi}^* \cos 2\phi \left[ -\frac{3}{2} |M_{1+}|^2 - 3 \operatorname{Re}(M_{1+}E_{1+}^*) \right] \\ & + \sqrt{2\epsilon(1+\epsilon)} \sin\theta_{\pi}^* \cos\phi \left[ -\operatorname{Re}(S_{0+}M_{1+}^*) - 6 \cos\theta_{\pi}^* \operatorname{Re}(S_{1+}M_{1+}^*) \right] \end{aligned}$$

From studying the  $\phi$  and  $\theta_{\pi}^*$  dependence of the cross section one can separate the term  $\operatorname{Re}(S_{1+}M_{1+}^*)$ , which is most sensitive to  $S_{1+}$ . Fig. 7 shows results of previous measurements<sup>14</sup>. The accuracy of existing data is clearly not sufficient to separate resonant and nonresonant parts. Note that the quantity  $\operatorname{Re}(S_{1+}M_{1+}^*)/|M_{1+}|^2$  is displayed. A resonance-like behaviour<sup>14</sup> of  $S_{1+}$  would result in a flat distribution in this quantity<sup>14</sup>. The  $Q^2=1 \text{ GeV}^2$  data show some  $W$  dependence which may indicate that the measured quantity contains nonresonant contributions. In order to enable a full determination of the resonant and nonresonant contribution to  $(S_{1+}M_{1+}^*)$ , a measurement of the term  $\operatorname{Im}(S_{1+}M_{1+}^*)$  is required<sup>14</sup> as well. This term is particularly sensitive to nonresonant contributions. If only  $S_{1+}$  and  $M_{1+}$  amplitudes of the resonance contribute, having the same phases, the term  $\operatorname{Im}(S_{1+}M_{1+}^*)$  would vanish identically. According to fixed and dispersion relation calculations the nonresonant contribution  $\operatorname{Re}S_{1+}$  ( $I=1/2$ ) may be of the same order of magnitude as  $\operatorname{Re}S_{1+}$  ( $I=3/2$ ). This would result in quite different phases for  $M_{1+}$  and  $S_{1+}$ , which consequently give rise to a sizeable polarization asymmetry in the vicinity of the resonance.

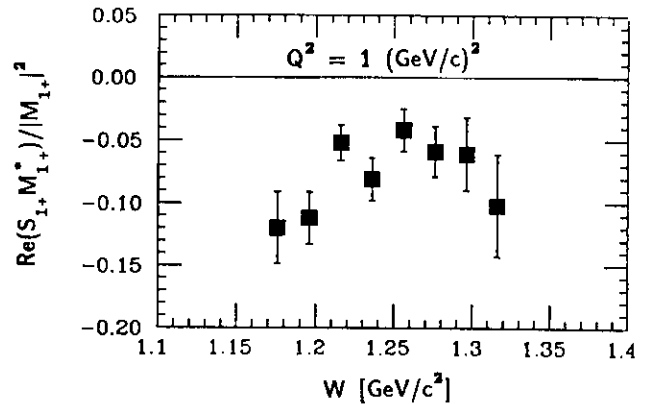


Fig. 7 The quantity  $\operatorname{Re}(S_{1+}M_{1+}^*)/|M_{1+}|^2$  in the  $\Delta(1232)$  region. Data from DESY<sup>14</sup>.

The quantity  $\operatorname{Im}(S_{1+}M_{1+}^*)$  can be measured by using a longitudinally polarized electron beam and measuring the cross section asymmetry<sup>16</sup>.

$$A_e \approx \sqrt{2\epsilon(1-\epsilon)} \sin\phi^* \sin\theta_{\pi}^* \left[ \operatorname{Im}(S_{0+}M_{1+}^*) + 6 \cos\theta_{\pi}^* \operatorname{Im}(S_{1+}M_{1+}^*) \right]$$

In this expression the same approximation as in the unpolarized cross section has been assumed. This experiment requires a measurement of the  $\theta_{\pi}^*$  distribution of one of the outgoing hadrons at large  $\phi$  (out of the scattering plane). Measuring the  $\theta_{\pi}^*$  dependence of  $A_e$  at fixed  $\sin\phi^*$  enables a separation of  $\operatorname{Im}(S_{0+}M_{1+}^*)$  and  $\operatorname{Im}(S_{1+}M_{1+}^*)$ . Asymmetries of 5 to 10% can be expected<sup>19</sup>.

## 5. Polarized Target Asymmetry in the Region of the $P_{11}(1440)$

There is an ongoing controversy as to whether or not the  $P_{11}(1440)$  is actually composed of two  $P_{11}$  resonances as a recent analysis indicates<sup>22</sup>. In electroproduction, however, only weak indications of a resonant structure in this particular mass region have been seen in unpolarized electroproduction experiments. Single pion photoproduction data have on the other hand revealed a rather strong resonance excitation<sup>22</sup>. Pion electroproduction may help solve the above controversy because of the additional kinematical degree of freedom given by  $Q^2$ . The various resonances may exhibit very different  $Q^2$  dependence.

Measurements of asymmetries with polarized targets appear quite sensitive to the strength of the  $P_{11}(1440)$  excitation. Fig. 8 shows the sensitivity of the target asymmetry in  $\pi^0$  production to the excitation of the  $P_{11}(1440)$ . By choosing a suitable orientation of the target polarization and by carefully selecting the kinematics of the decay particles, interference effects may become large and exhibit sizable effects even from weak resonances. In this example the amplitudes which have been obtained in an analysis<sup>22</sup> of the world data at  $Q^2=1 \text{ GeV}^2$  were used. In the analysis, a sizable longitudinal amplitude  $S_+$  was found for the  $P_{11}(1440)$ . This gives rise to strong effects in  $T_z$  which contains transverse-longitudinal interference terms.

Target Polarization Asymmetry  $T_z(\gamma p \rightarrow p \pi^0)$  at  $Q^2=1(\text{GeV}/c)^2$   
( $\phi = \pi/2$ ;  $\theta_\pi^* = 10^\circ$ )

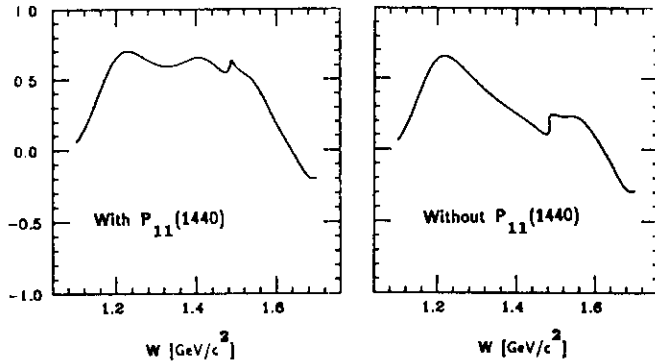


Fig. 8 Polarized target asymmetry  $T_z(\gamma p \rightarrow p \pi^0)$  for a specific kinematical situation. The target protons are polarized perpendicular to the virtual photon direction, in the electron scattering plane. Results of a recent analysis<sup>22</sup> have been used to predict the asymmetry (l.h.s.). To illustrate the sensitivity to the longitudinal coupling of the  $P_{11}$ , the expected asymmetry is shown if the  $P_{11}$  were not excited (r.h.s.).

## 6. Double Polarization Asymmetry

With a polarized beam and a polarized nucleon target, one can measure double polarization asymmetries which require flipping the spin of the electron as well as of the target nucleons. Of particular interest is the asymmetry  $D_z$ .

$$D_z = \frac{\sigma(P_z=1, P_e=1) - \sigma(P_z=1, P_e=-1) - \sigma(P_z=-1, P_e=1) + \sigma(P_z=-1, P_e=-1)}{\sigma(P_z=1, P_e=1) + \sigma(P_z=1, P_e=-1) + \sigma(P_z=-1, P_e=1) + \sigma(P_z=-1, P_e=-1)}$$

where the nucleon spin is aligned parallel and antiparallel to the direction of the virtual photon. Fig. 9 shows that this asymmetry can be large.  $D_z$  measures directly the helicity asymmetry

$$\frac{1}{2\pi} \int D_z(Q^2, W, \theta_\pi^*, \phi) d\phi = \frac{\sigma_{1/2}^T - \sigma_{3/2}^T}{2\sigma_0}$$

for the transverse cross section. The partial wave analysis of this quantity at fixed  $Q^2$  and  $W$  yields the helicity asymmetry for single partial waves. Unpolarized measurements allow the determination of  $\sigma_{1/2}^T + \sigma_{3/2}^T$  for single partial waves. The two measurements combined allow determination of  $\sigma_{1/2}^T \sim |A_{1/2}|^2$  and  $\sigma_{3/2}^T \sim |A_{3/2}|^2$  for specific resonances (after subtracting the nonresonant background).  $A_{1/2}$  and  $A_{3/2}$  have been predicted by microscopic models of the nucleon and provide tests of the helicity structure of the resonance transition. In view of the quark model and QCD predictions, e.g., that  $\sigma_{3/2}^T$  should vanish at large  $Q^2$ , measurements of this type provide immediate tests of essential aspects of theoretical approaches in the nonperturbative regime. In Fig. 9 examples of predictions for  $D_z$  are shown.

Double Polarization Asymmetry  $D_z(\gamma p \rightarrow p \pi^0)$  at  $Q^2=1(\text{GeV}/c)^2$

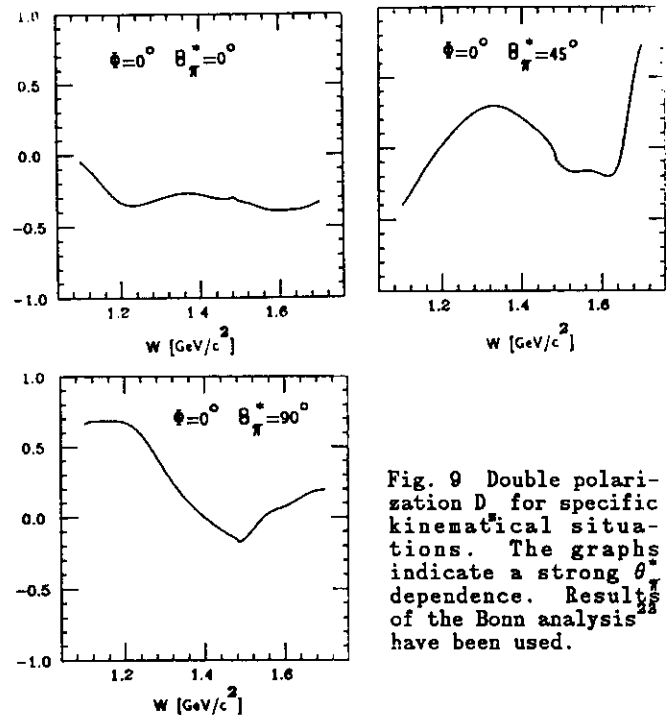


Fig. 9 Double polarization  $D_z$  for specific kinematical situations. The graphs indicate a strong  $\theta_\pi^*$  dependence. Results<sup>22</sup> of the Bonn analysis have been used.

## IV. Parity Violation Measurement in the $\Lambda(1232)$ Region

In low energy ( $Q^2 \ll M_\pi^2$ ) neutral current interactions, the parity violating contribution arises from the interference between the one-photon exchange and the neutral weak boson ( $Z^0$ ) exchange graphs. In electron scattering, the interaction contains an isoscalar as well as an isovector piece in both the vector ( $V_\mu$ ) and axial vector ( $A_\mu$ ) coupling. The effective Lagrangian which describes the parity non-conserving (PNC) part of the interaction for electron hadron scattering is given by<sup>24</sup>

$$L_{\text{eff}}^{\text{PNC}} = -\frac{G_F}{\sqrt{2}} \cdot \left[ \bar{e} \gamma_\mu \gamma_5 e (\tilde{\alpha} V_\mu^3 + \tilde{\gamma} V_\mu^0) + \bar{e} \gamma_\mu e (\tilde{\beta} A_\mu^3 + \tilde{\delta} A_\mu^0) \right]$$

The  $\tilde{\alpha}$ ,  $\tilde{\beta}$ ,  $\tilde{\delta}$ ,  $\tilde{\gamma}$  denote the respective coupling constants which have to be determined experimentally. In the

Glashow-Salam-Weinberg Model (GSW) of electroweak interaction, these coupling constants can be expressed in terms of a single parameter, the weak mixing angle  $\theta_w$ . By choosing appropriate kinematical conditions for electron scattering from nucleons and nuclear targets, one can determine the couplings by a set of four linearly independent measurements.

The SLAC/Yale  $D(e, e')X$  scattering experiment<sup>35</sup>, in conjunction with atomic physics experiments<sup>38</sup>, enabled a model independent determination of  $\alpha$ ,  $\gamma$ . The Mainz experiment<sup>36</sup> measures a different combination of the four coupling constants and allows the extraction of a combination of  $\beta$  and  $\delta$ , using the previously obtained results as an input. It should, however, be noted that this experiment measures quasielastic electron scattering from  $^9\text{Be}$  rather than elastic electron nucleon scattering. This fact could be of importance if the data are used for a determination of the weak angle. The Bates experiment<sup>36</sup>, which has recently become operational, simply measures  $\gamma$ .

From this brief survey of existing measurements it is obvious that for a complete determination of the coupling constants additional measurements are needed. One should also attempt to measure a possible  $Q^2$  dependence of these couplings. Deviations from the GSW model may occur at the level of one percent<sup>39</sup>. High precision measurements are therefore needed.

Various arguments have been made for measuring parity violation in elastic electron-proton scattering<sup>30,32</sup>. A precise measurement of the  $\Lambda$ -excitation seems equally important. We summarize here some arguments for measuring this process.

- $\Lambda(1232)$  excitation separates the isovector part ( $\alpha, \beta$ ).
- It is an almost pure magnetic resonance with a dominant magnetic dipole ( $M_{1+}$ ) excitation. The scalar coupling ( $S_{1+}$ ) and the electric coupling ( $E_{1+}$ ) are both small.
- At low  $Q^2$  ( $< 0.6 \text{ GeV}^2$ ) the nonresonant background is small. Its effects on the PNC asymmetry should be reliably calculable<sup>32</sup>. In order to understand the PNC effects of the nonresonant part at the one percent level, more precise electroproduction data in different isospin channels will presumably be needed as well.
- The asymmetry is predicted to be large in the GSW model<sup>31,34</sup>.

$$A_{\Lambda(1232)} = \left( \frac{G_F}{\sqrt{2}} \right) \left( \frac{Q^2}{2\pi\alpha} \right) [\tilde{\alpha} + F(Q^2, E)\tilde{\beta}]$$

and has a strong sensitivity to  $\sin^2\theta_w$ .

The factor  $F(Q^2, E)$  in the above formula is close to 1 in the energy range of interest. Assuming a weak angle of  $\sin^2\theta_w = 0.225$ , one obtains  $A_{\Lambda(1232)} \sim -1.17 \times 10^{-4} Q^2$ .

## V. Conclusions

Polarization experiments open up a large variety of possibilities to study electromagnetic properties of the nucleon and its excited states with increased sensitivity compared to unpolarized measurements. The numerical examples chosen assumed an external target situation at CEBAF energies. Most of the experiments can, of course, be done with gas targets in storage rings, if high enough luminosities can be achieved. "High enough" translates as  $\geq 10^{32} \text{ cm}^{-2} \text{ sec}^{-1}$  for the measurement of the neutron electric formfactor and  $\geq 10^{34} \text{ cm}^{-2} \text{ sec}^{-1}$  for the proton electric formfactor. The

nucleon resonance program would also need luminosities in excess of  $10^{34} \text{ cm}^{-2} \text{ sec}^{-1}$  for a substantial improvement of previous work, if full solid angle coverage is provided.

Precision experiments for studying parity violation in electron scattering require measurements with very high luminosity ( $L > 10^{30} \text{ cm}^{-2} \text{ sec}^{-1}$ ) and large acceptance detectors<sup>35,36</sup>. Because of the luminosity requirements, these experiments will have to employ thick targets in an external beam line.

## References

- 1) S. Galster et al., Nucl. Phys. B32 (1971) 221.
- 2) W. Bartel et al., Nucl. Phys. B58 (1973) 429.
- 3) R. Arnold, C. Carlson, F. Gross, Phys. Rev. C23 (1981) 383.
- 4) V. Burkert, Lect. Notes in Phys. 234 (1984) 228.
- 5) W. A. Nesterenko, A. V. Radyushkin, Phys. Lett. 115B (1982) 410.
- 6) K. H. Althoff et al., Europhysics Conf. on Nuclear Physics with Electromagnetic probes, Paris (1985).
- 7) T. O. Niinikoski, Proc. 4th Workshop on Polarized Target Materials and Techniques, ed. W. Meyer, Bonn (1984).
- 8) W. Meyer et al., Nucl. Instr. Methods A244 (1986) 574.
- 9) V. Burkert, CEBAF Reports CR-86-002, CR-86-003, CR-86-011.
- 10) U. Hartfiel et al., Proc. 4th Workshop on Polarized Target Materials and Techniques, Bonn (1984).
- 11) W. Pfeil, Report of the 1986 Summer Study Group, CEBAF, Newport News, Virginia, 219.
- 12) F. Foster and G. Hughes, Rep. Prog. Phys. 46 (1983) 1445.
- 13) D. Walecka, Acta Physica Polonica B3 (1972) 117.
- 14) R. Walker, Phys. Rev. 182 (1969) 1729.
- 15) A. Bartl, W. Majeotto, Nucl. Phys., B62 (1973) 267.
- 16) H. Funsten, Report of the 1986 Summer Study Group, CEBAF, Newport News, Virginia, 183.
- 17) C. Carlson, Phys. Rev. D34 (1980) 2704.
- 18) N. Isgur, G. Karl, Phys. Rev. D19 (1979) 7653; Phys. Rev. D23 (1981) 817.
- 19) M. Bourdeau, N. C. Mukhopadhyay, Phys. Rev. Lett. 58 (1987) 976.
- 20) G. V. Gehlen, Nucl. Phys. B26 (1971) 141.
- 21) R. Arndt, J. Ford, D. Roper, Phys. Rev. D32 (1985) 1085.
- 22) R. L. Crawford, W. T. Morton, Nucl. Phys. B211 (1983) 1.
- 23) B. Boden and G. Kroesen, Report of the 1986 Summer Study Group, CEBAF, Newport News, Virginia.
- 24) P. Q. Hung, J. J. Sakurai, Phys. Lett. 63B (1976) 295.
- 25) C. Y. Prescott et al., Phys. Lett. 77B (1978) 347; Phys. Lett., 84B (1979) 524.
- 26) P. Q. Hung, J. J. Sakurai, Annual Rev. of Nucl. & Part. Science 31.
- 27) W. Achenbach et al., Presented at the Int. Symp. on High Energy Spin Physics, Protvino, Sept. 1986.
- 28) Proceedings of CEBAF Workshop on Parity Violation, Newport News, VA, Dec. 1986, ed. R. Siegel.
- 29) S. Kowalski, in (28).
- 30) P. Langacker, in (28).
- 31) D. Walecka, in (28); see also D. Walecka, Argonne Lecture Notes ANL-83-50 (1983).
- 32) S. Pollock, in (28).
- 33) S. Pollock, private communications.
- 34) D. Jones, S. Petcov, Phys. Lett. 91B (1980) 137.
- 35) V. Burkert, in (28).
- 36) B. Mecking, in (28).
- 37) J. C. Alder et al., Nucl. Phys. B46 (1972) 573.